Inorg. Chem. **2009**, *48*, 2748−2759

Inorganic Chemistry

Article

Linear M≡E−Me Versus Bent M−E−Me: Bonding Analysis in Heavier Metal-ylidyne Complexes $[(Cp)(CO)_2M{\equiv}EMe]$ and Metallo-ylidenes $[(Cp)(CO)_3M{-}EMe]$ (M = Cr, Mo, W; E = Si, Ge, Sn, Pb)

Krishna K. Pandey*,[†] **and Agustí Lledós***,[‡]

School of Chemical Sciences, Devi Ahilya University Indore, Indore, India 452017, and
Departament de Química, Universitat Autònoma de Barcelona,
08193 Bellaterra, Barcelona, Spain

Received June 11, 2008

The electronic and molecular structures of the complexes $[(\eta^5\text{-}C_5H_5)(CO)_2M{\equiv}EMe]$ and $[(\eta^5\text{-}C_5H_5)(CO)_3M{-}EMe]$ (M = Cr, Mo, W; E = Si, Sn, Pb) are calculated at the density-functional theory (DFT) level using the exchange correlation functionals B3LYP and BP86. The theoretically predicted bond lengths and angles of the model compounds are in excellent agreement with experimental values. The calculations reveal the presence of a strong M≡E triple ($\sigma + 2\pi$) bond in $[(\eta^5\text{-}C_5H_5)(CO)_2M{\equiv}EMe]$. The M−E bond lengths in $[(\eta^5\text{-}C_5H_5)(CO)_3M{-}EMe]$ are longer than those expected for a single bond. The nature of the M≡EMe and M−EMe interactions was analyzed with charge and energy decomposition methods. In the M≡EMe bond, the M−E σ-bonding orbitals are always polarized toward the silicon, tin, and lead atoms, and the polarization increases from chromium to tungsten. In contrast, in the M−EMe bond, the M−E σ-bonding orbitals are significantly polarized toward the metal atom. The hybridization at the metal atoms in the M≡E bonds has d character in the range 60.6−68.8%, while in the M−E bonds has large d character which is always >86% of the total atomic orbital contribution. In the complexes $[(\eta^5\text{-}C_5H_5)(CO)_2M{\equiv}EMe]$, the contributions of the electrostatic interactions, ΔE_{elstat}, and the covalent bonding, ΔE_{orb}, have nearly the same values for silylidyne and germylidyne complexes, while for the stannylidyne and plumbylidyne complexes, the electrostatic interactions, ΔE_{elstat}, are greater than the orbital interaction, ΔE_{orb}. The covalent bonding has a high degree of π-character. The total interaction energy ΔE_{int} in the compound $[(\eta^5\text{-}C_5H_5)(CO)_3M{-}EMe]$ is less attractive than those in the complexes $[(\eta^5\text{-}C_5H_5)(CO)_2M{\equiv}EMe]$. The M−ER bonds have a slightly lower degree of covalent bonding (34.9−44.9%) than the M≡EMe bonds (42.1−50.2%). The drastic difference between the two classes of compounds are found for the degree of a″ (π) bonding. The contribution of ΔE_π to the covalent term ΔE_{orb} is much higher in the M≡EMe bonding (41.6−42.6%) than in the M−EMe bonding (17.1−20.4%). While the π bonding contribution in $[(\eta^5\text{-}C_5H_5)(CO)_3M{-}EMe]$ are weaker than those in $[(\eta^5\text{-}C_5H_5)(CO)_2M{\equiv}EMe]$, the σ-bonding contribution in the former compounds are stronger than those in the latter.

Introduction

The chemistry of transition metal complexes with terminal carbyne (CR) ligands has blossomed in the last thirty years during which much knowledge of their properties has been obtained.[1−10] In sharp contrast to the transition metal carbyne complexes, coordination chemistry of heavier analogues with ligands ER (E = Si, Ge, Sn, Pb) has been much less developed. Tilley et al. reported the first structurally characterized complex with silylyne character $[(\eta^5\text{-}C_5Me_5)(dmpe)(H)Mo{\equiv}SiMes]([B(C_6F_5)_4]$ (dmpe = $Me_2PCH_2CH_2PMe_2$).[11] The previously reported complex $[(\eta^5\text{-}C_5Me_5)$-

---

* To whom correspondence should be addressed. E-mail: kkpandey.schem@dauniv.ac.in (K.K.P.), agusti@klingon.uab.es (A.L.).

[†] Devi Ahilya University Indore.

[‡] Universitat Autònoma de Barcelona.

(1) Nugent, W. A.; Mayer, J. M. *Metal-Ligand Multiple Bonds*; Wiley; New York, 1988.

(2) Fisher, H.; Hoffman, P.; Kreisal, F. R.; Schrock, R. R.; Schubert, U.; Weiss, K. *Carbyne Complexes*; VCH; New York, 1988.

(3) *Transition Metal Carbyne Complexes*; Kreisel, F. R., Ed.; Kluwer; Dordrecht, The Neitherlands, 1993.

(4) Lapointe, A. M.; Schrock, R. R.; Davis, W. M. *J. Am. Chem. Soc.* **1995**, *117*, 4802.

(5) Vyboishchikov, S. F.; Frenking, G. *Chem.−Eur. J.* **1998**, *4*, 1439.

10.1021/ic801072g CCC: $40.75

$(\mathrm{PMe_3})_2\mathrm{Ru}\{\mathrm{Si(bipy)(SC_6H_4\text{-}4\text{-}Me)}\}][\mathrm{OTf}]_2$ can be formally described as a silylyne complex which has four coordinated silicon.[12] The first compounds containing triple bonds to a group 14-element (germanium) were the transition metal complexes $[(\eta^5\text{-}\mathrm{C_5H_5})(\mathrm{CO})_2\mathrm{M{\equiv}GeR}]$ (M = Cr, Mo, W).[13,14] Filippou et al. reported another class of germylidyne complexes $[\mathrm{X(L)_2M{\equiv}GeCp^*)}]$ (L = dppe, depe; X = Cl, Br; M = Mo, W), $[\mathrm{X(dppe)_2W{\equiv}GeCp^*)}]$ (X = H, CN, NCO, NCS, $\mathrm{N_3}$) and $[\mathrm{X(PMe_3)_4M{\equiv}Ge{-}R)}]$ (X = Cl, I, H, NCS).[15−19] Recently, Filippou and co-workers isolated the first representative examples of stannylidyne[20,21] complexes *trans*-$[\mathrm{Cl(PMe_3)_4W{\equiv}SnR}]$, $[\mathrm{Cl(dppe)_2W{\equiv}SnR}]$ and $[\mathrm{(dppe)_2W{\equiv}SnR}][\mathrm{PF_6}]$ (R = $\mathrm{C_6H_3\text{-}2,6\text{-}Mes_2}$) and plumbylidyne complexes $[\mathrm{Br(PMe_3)_4Mo{\equiv}Pb{-}C_6H_3\text{-}2,6\text{-}Trip_2}]$,[22] $[\mathrm{X(PMe_3)_4W{\equiv}Pb{-}R)}]$ (X = Br, I),[23] $[\mathrm{L(PMe_3)_4W{\equiv}Pb\text{-}R)}]^+$ (L = $\mathrm{PMe_3}$, PhCN),[23] and $[\mathrm{H(PMe_3)_4W{\equiv}Pb{-}R)}]$.[24] A characteristic feature of these silylidyne, germylidyne, stannylidyne, and plumbylidyne complexes is that the M−E−R linkages are nearly linear. Chart 1 gives an overview of silylidyne, germylidyne, stannylidyne, and plumbylidyne complexes that have been reported in the literature.

Recently, compounds [M]ER (E = Ge, Sn, Pb), which have a strongly bent M−E−R linkage (Chart 2), were synthesized and structurally characterized. The compounds should be considered as derivatives of silylidenes, :SiR2, stannylidenes, :SnR2 and plumbylidenes, :PbR2, that is, they are metallosilylidenes, metallostannylidenes, and metalloplumbylidenes. Jutzi and Leue[25] isolated the first metallogermylidene derivatives of iron $[(\eta^5\text{-}\mathrm{C_5R_5})(\mathrm{CO})_2\mathrm{Fe\text{-}GeC_6H_2\text{-}2,4,6\text{-}tBu_3}]$ (R = H, Me), but no structures have been determined. Power et al. reported first structurally characterized representative examples of metallogermylidenes, metallostannylidenes, and metalloplumbylidenes (Chart 2).[26,27] The M−E−R bond angles in these complexes are between 106.7° and 117.8°. It is worth to point out that the related metallocarbenes and metallosilylenes are still unknown. This is probably related to the instability of carbenes and silylenes. A number of carbenes being stabilized,[28−37] it seems feasible that related metallocarbenes could be isolated. There has been considerable interest in the synthesis, structure, bonding, and reactivities of monomeric heavy group 14-element analogues of carbenes, that is, silylidenes, germylidenes, stannylidenes, and plumbylidenes.[38−49]

The electronic structure and bonding situation of transition metal carbyne complexes have been investigated in several theoretical studies,[3,6,7] but relatively little attention has been paid to metal-germylidyne, metal-stannylidyne, and metal-plumbylidyne complexes.[15,18,21−23,50,51] We have reported the differences between the chemical bonding situation of metal-germylidyne complexes with metallogermylidenes.[52] In the present paper, nine complexes with linear M−E−Me linkage, $[(\eta^5\text{-}\mathrm{C_5H_5})(\mathrm{CO})_2\mathrm{M{\equiv}EMe}]$ (**Ia**, M = Cr, E = Si; **Ib**, M = Cr, E = Sn; **Ic**, M = Cr, E = Pb; **Id**, M = Mo, E = Si; **Ie**, M = Mo, E = Sn; **If**, M = Mo, E = Pb; **Ig**, M = W, E = Si; **Ih**, M = W, E = Sn; **Ii**, M = W, E = Pb) and nine compounds having bent M−E−Me linkage, $[(\eta^5\text{-}\mathrm{C_5H_5})(\mathrm{CO})_3\mathrm{M{-}EMe}]$ (**IIa**, M = Cr, E = Si; **IIb**, M = Cr,

---

(6) Frenking, G.; Fröhlich, N. *Chem. Rev.* **2000**, *100*, 717.
(7) Choi, S. K.; Gal, Y. S.; Jin, S. H.; Kim, H. K. *Chem. Rev.* **2000**, *100*, 1645.
(8) Herndon, J. W. *Coord. Chem. Rev.* **2002**, *227*, 1.
(9) Cotton, F. A.; Wilkinson, G.; Murillo, C. A.; Bochmann, M. *Advanced Inorganic Chemistry*, 6th ed.; Wiley: New York, 1999.
(10) Herndon, J. W. *Coord. Chem. Rev.* **2006**, *250*, 1889.
(11) Mork, B. V.; Tilley, T. D. *Angew. Chem., Int. Ed.* **2003**, *42*, 357.
(12) Grumbine, S. D.; Chadha, R. K.; Tilley, T. D. *J. Am. Chem. Soc.* **1992**, *114*, 1518.
(13) Simons, R. S.; Power, P. P. *J. Am. Chem. Soc.* **1996**, *118*, 11966.
(14) Pu, L.; Twamley, B.; Haubrich, S. T.; Olmstead, M. M.; Mork, B. V.; Simons, R. S.; Power, P. P. *J. Am. Chem. Soc.* **2000**, *122*, 650.
(15) Filippou, A. C.; Philippopoulos, A. I.; Portius, P.; Neumann, D. U. *Angew. Chem., Int. Ed.* **2000**, *39*, 2778.
(16) Filippou, A. C.; Portius, P.; Philippopoulos, A. I. *Organometallics* **2002**, *21*, 653.
(17) Filippou, A. C.; Philippopoulos, A. I.; Portius, P.; Schnakenburg, G. *Organometallics* **2004**, *23*, 4503.
(18) Filippou, A. C.; Schnakenburg, G.; Philippopoulos, A. I.; Weidemann, N. *Angew. Chem., Int. Ed.* **2005**, *44*, 5979.
(19) Filippou, A. C.; Schnakenburg, G.; Weidemann, N.; Philippopoulos, A. I. *Angew. Chem., Int. Ed.* **2006**, *45*, 5987.
(20) Filippou, A. C.; Portius, P.; Philippopoulos, A. I.; Rohde, H. *Angew. Chem., Int. Ed.* **2003**, *42*, 445.
(21) Filippou, A. C.; Philippopoulos, A. I.; Schnakenburg, G. *Organometallics* **2003**, *22*, 3339.
(22) Filippou, A. C.; Rohde, H.; Schnakenburg, G. *Angew. Chem., Int. Ed.* **2004**, *43*, 2243.
(23) Filippou, A. C.; Weidemann, N.; Schnakenburg, G.; Rohde, H.; Philippopoulos, A. I. *Angew. Chem., Int. Ed.* **2004**, *43*, 6512.
(24) Filippou, A. C.; Schnakenburg, G.; Weidemann, N. *Angew. Chem., Int. Ed.* **2008**, *47*, 5799.
(25) Jutzi, P.; Leue, C. *Organometallics* **1994**, *13*, 2898.
(26) Eichler, B. E.; Phillips, A. D.; Haubrich, S. T.; Mork, B. V.; Power, P. P. *Organometallics* **2002**, *21*, 5622.
(27) Pu, L.; Power, P. P.; Boltes, I.; Herbst-Irmer, R. *Organometallics* **2000**, *19*, 352.
(28) Arduengo, A. J.; Harlow, R. L.; Kline, M. *J. Am. Chem. Soc.* **1991**, *113*, 361.
(29) Arduengo, A. J. *Acc. Chem. Res.* **1999**, *32*, 913.
(30) Bourissou, D.; Guerret, O.; Gabbai, F. P.; Bertrand, G. *Chem. Rev.* **2000**, *100*, 39.
(31) Herrmann, W. A. *Angew. Chem., Int. Ed.* **2002**, *41*, 1290.
(32) Merceron, N.; Miqueu, K.; Baceiredo, A.; Bertrand, G. *J. Am. Chem. Soc.* **2002**, *124*, 6806.
(33) Despagnet-Ayoub, E.; Solé, S.; Gornitzka, H.; Rozhenko, A. B.; Schoeller, W. W.; Bourissou, D.; Bertrand, G. *J. Am. Chem. Soc.* **2003**, *125*, 124.
(34) Otto, M.; Conejero, S.; Canac, Y.; Romanenko, V. D.; Rudzevitch, V.; Bertrand, G. *J. Am. Chem. Soc.* **2004**, *126*, 1016.
(35) Cattoen, X.; Gornitzka, H.; Bourissou, D.; Bertrand, G. *J. Am. Chem. Soc.* **2004**, *126*, 1342.
(36) Lavallo, V.; Mafhouz, J.; Canac, Y.; Donnadieu, B.; Schoeller, W. W.; Bertrand, G. *J. Am. Chem. Soc.* **2004**, *126*, 8670.
(37) Kirmse, W. *Angew. Chem., Int. Ed.* **2004**, *43*, 1767.
(38) Lappert, M. F.; Rowe, R. S. *Coord. Chem. Rev.* **1990**, *100*, 267.
(39) Barrau, J.; Rima, G. *Coord. Chem. Rev.* **1998**, *178−180*, 593.
(40) Weidenbruch, M. *Eur. J. Inorg. Chem.* **1999**, 373.
(41) Power, P. P. *Chem. Rev.* **1999**, *99*, 3463.
(42) Jutzi, P. *Angew. Chem., Int. Ed.* **2000**, *39*, 3797, and references therein.
(43) Massey, A. G. *Main Group Chemistry*, 2nd ed.; Wiley: Chichester, U.K., 2000.
(44) Tokitoh, N.; Okazaki, R. *Coord. Chem. Rev.* **2000**, *210*, 251.
(45) Pu, L.; Twamley, B.; Power, P. P. *J. Am. Chem. Soc.* **2000**, *122*, 3524.
(46) Phillips, A. D.; Wright, R. J.; Olmstead, M. M.; Power, P. P. *J. Am. Chem. Soc.* **2002**, *124*, 5930.
(47) Stender, M.; Phillips, A. D.; Wright, R. J.; Power, P. P. *Angew. Chem., Int. Ed.* **2002**, *41*, 1785.
(48) Weidenbruch, M. *Angew. Chem., Int. Ed.* **2003**, *42*, 2222.
(49) Tokitoh, N.; Ando, W. *Reactive Intermediate Chemistry*; Moss, R. A., Platz, M. S., Jones, M., Jr., Eds.; John Wiley & Sons Inc.: Hoboken, NJ, 2004; p 651.
(50) Lein, M.; Szabo, A.; Kovacs, A.; Frenking, G. *Faraday Soc. Discuss.* **2003**, *124*, 365.
(51) Tagaki, N.; Yamazaki, K.; Nagase, S. *Bull. Korean Chem. Soc.* **2003**, *24*, 832.
(52) Pandey, K. K.; Lein, M.; Frenking, G. *J. Am. Chem. Soc.* **2003**, *125*, 1660.

Chart 1. Overview of Experimentally Known Silylidyne, Germylidyne, Stannylidyne, and Plumbylydine Complexes

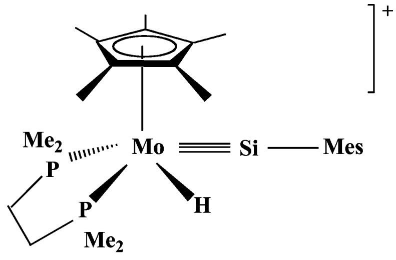

Mo-Si = 2.219 (2) Å

<Mo-Si-C(Mes) = 170.9(2)°

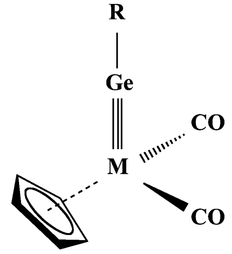

R= Ar* = 2,6-bis(2,4,6-trimethylphenyl)phenyl
R= Ar = 2,6-bis(2,4,6-triisopropylphenyl)phenyl**

	M-Ge Å	Ge-C Å	M-Ge-C
$[(Cp)(CO)_2Cr(GeAr^{**})]$	2.1666(4)	1.9512(18)	175.99(6)°
$[(Cp)(CO)_2Mo(GeAr^{**})]$	2.272(8)	1.936(5)	174.25(14)°
$[(Cp)(CO)_2Mo(GeAr^{*})]$	2.271(1)	1.933(7)	172.2(2)°
$[(Cp)(CO)_2W(GeAr^{*})]$	2.2767(14)	1.916(11)	170.9(3)°

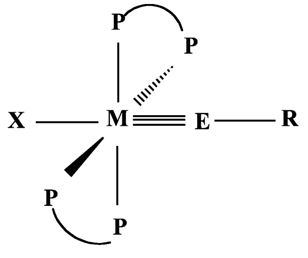

	M-E Å	E-C Å	M-E-C
$[Cl(dppe)_2Mo(GeCp^*)]$	2.3185(6)	2.049(4)	172.0(1)°
$[Br(dppe)_2Mo(GeCp^*)]$	2.3103(6)	2.029(5)	171.6(2)°
$[Cl(dppe)_2W(GeCp^*)]$	2.302(1)	2.038(5)	172.2(2)°
$[Br(dppe)_2W(GeCp^*)]$	2.293(1)	2.030(8)	172.4(2)°
$[I(dppe)_2W(GeCp^*)]$	2.3060(9)	2.049(6)	172.6(2)°
$[H(dppe)_2W(GeCp^*)]$	2.310(1)	2.037(4)	176.8(1)°
$[(NCO)(dppe)_2W(GeCp^*)]$	2.2991(9)	2.031(5)	172.0(1)°
$[(CN)(dppe)_2W(GeCp^*)]$	2.3184(6)	2.008(4)	172.2(1)°
$[(MeCN)(dppe)_2W(GeCp^*)]^+$	2.3030(8)	2.004(2)	174.31(7)°
$[Br(depe)_2Mo(GeCp^*)]$	2.2798(5)	2.046(3)	177.46(8)°
$[H(PMe_3)_4W(GeAr^{**})]$	2.324(1)	1.977(6)	178.9(2)°
$[Cl(PMe_3)_4W(GeAr^{**})]$	2.338(1)	1.982(10)	177.9(3)°
$[I(PMe_3)_4W(GeAr^{**})]$	2.3206(4)	2.004(2)	175.79(3)°
$[(dppe)_2W(SnAr^*)]^+$	2.4641(7)	2.146(3)	178.77(9)°
$[Cl(PMe_3)_4W(SnAr^*)]$	2.4901(7)	2.179(5)	178.2(1)°
$[Br(PMe_3)_4Mo(PbAr^{**})]$	2.5495(8)	2.277(7)	177.8(2)°
$[Br(PMe_3)_4W(PbAr^{**})]$	2.5464(5)	2.254(6)	177.5(2)°
$[I(PMe_3)_4W(PbAr^{**})]$	2.5477(3)	2.258(3)	175.79(8)°
$[H(PMe_3)_4W(PbAr^{**})]$	2.5525(3)	2.229(6)	178.7(2)°
$[(PhCN)(PMe_3)_4W(PbAr^{**})]^+$	2.5520(6)	2.228(5)	171.7(1)°
$[(PMe_3)_5W(PbAr^{**})]^+$	2.5744(2)	2.289(4)	178.7(2)°

E = Sn; **IIc**, M = Cr, E = Pb; **IId**, M = Mo, E = Si; **IIe**, M = Mo, E = Sn; **IIf**, M = Mo, E = Pb; **IIg**, M = W, E = Si; **IIh**, M = W, E = Sn; **IIi**, M = W, E = Pb) have been investigated at the density-functional theory (DFT) level using BP86 and B3LYP functionals. Results of the previous calculations[52] on metal-germylidyne and metallogermylidenes have been included. In the model complexes, the bulky substituents at silicon, germanium, tin, and lead atoms are replaced by a methyl group.

The main goals of the present study are (i) to investigate the structures and to analyze the nature of M−E bonds in silylidyne, stannylidyne, plumbylidyne complexes and metallosilylidenes, metallostannylidenes, metalloplumbylidenes, (ii) to provide a quantitative difference of the bonding between the linear [M≡E−R] and the bent [M−E−R] coordination modes, and (iii) to investigate the contributions of the M−ER σ-bonding and M−ER π-bonding to the total M≡ER and M−ER bonding energies. To this end we report on the energy decomposition analysis of the M≡ER and M−ER bonds which gives the energies that are associated with the M≡ER σ-donation and M → ER π-bonding. The relative strength of the electrostatic and covalent contributions to the bond strength will also be reported. We investigate the influence of the variation of the group 14-element on the nature of the transition metal main group triple and single bonds. A comparison of the calculated Bond Dissociation Energies (BDEs) with the previous values reported in the literature is also presented.

Computational Methods

Calculations of all complexes have been performed using the hybrid B3LYP density functional method, which uses Becke's 3-parameter nonlocal exchange functional[53] mixed with the exact (Hartree−Fock) exchange functional and Lee−Yang−Parr's nonlocal correlation functional.[54] The geometries of the complexes

---

(53) Becke, D. *J. Chem. Phys.* **1993**, *98*, 5648.
(54) Lee, C.; Yang, W.; Parr, R. G. *Phys. Rev. B* **1988**, *37*, 785.

Chart 2. Overview of Experimentally Known Heavy Metallo-ylidenes

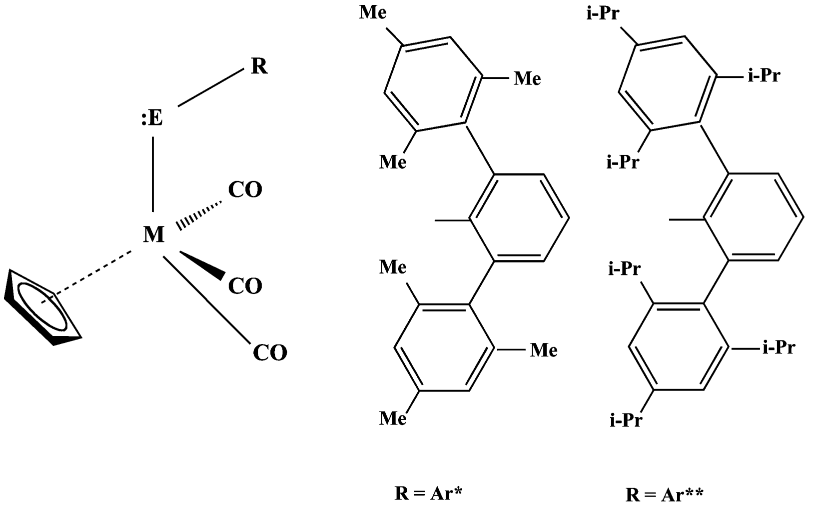

Ar* = 2,6-bis(2,4,6-trimethylphenyl)phenyl
Ar** = 2,6-bis(2,4,6-triisopropylphenyl)phenyl

	M-E Å	E-C(R) Å	M-E-C(R)
$[(Cp)(CO)_3Cr\text{-}GeAr^{**}]$	2.590(2)	1.989(8)	117.8(2)°
$[(Cp)(CO)_3W\text{-}GeAr^{**}]$	2.681(3)	1.99(2)	114.7(6)°
$[(Cp)(CO)_3Cr\text{-}SnAr^{*}]$	2.816(3)	2.140(19)	111.0(4)°
$[(Cp)(CO)_3Mo\text{-}SnAr^{*}]$	2.9045(10)	2.204(4)	106.7(10)°
$[(Cp)(CO)_3W\text{-}SnAr^{*}]$	2.9107(10)	2.200(9)	110.8(2)°
$[(Cp)(CO)_3Cr\text{-}SnAr^{**}]$	2.8474(7)	2.214(4)	110.12(9)°
$[(Cp)(CO)_3Mo\text{-}SnAr^{**}]$	2.8960(9)	2.191(3)	110.14(10)°
$[(Cp)(CO)_3W\text{-}SnAr^{**}]$	2.9030(8)	2.185(8)	109.9(2)°
$[(Cp)(CO)_3Cr\text{-}PbAr^{**}]$	2.9092(9)	2.294(4)	113.58(9)°
$[(Cp)(CO)_3Mo\text{-}PbAr^{**}]$	2.9845(7)	2.291(5)	110.00(13)°
$[(Cp)(CO)_3W\text{-}PbAr^{**}]$	2.9809(10)	2.283(7)	108.6(2)°

$[(\eta5\text{-}C_5H_5)(CO)_2M{\equiv}EMe)]$ and compounds $[(\eta5\text{-}C_5H_5)(CO)_3M{-}EMe)]$ (M = Cr, Mo, W; E = Si, Sn, Pb) were optimized using C_s symmetry constraints. with standard 6-311G(d) basis sets[55,56] for H, C, O, and Si atoms. For Cr, Mo, and W quasi-relativistic effective core potentials (ECP) determined by Hay and Wadt have been used.[57] The valence basis sets for Cr, Mo, and W have triple-ζ quality (10s10p5d1f/3s3p3d1f) which include (n+1)p functions,[58] augmented by an additional set of f orbitals with an exponent of 1.941 for Cr, 1.043 for Mo, and 0.823 for W.[59] For tin and lead, the standard (3s4p1d/2s3p1d) valence basis functions of Hay and Wadt have been used.[60] This basis set is denoted TZP. Frequency calculations were performed at B3LYP/TZP to determine whether the optimized geometries were minima on the potential energy surface. The electronic structures of the complexes were examined by NBO analysis.[61] The B3LYP/TZP calculations were carried out with the Gaussian98 program.[62] All MO pictures were made by using the MOLDEN program.[63]

Calculations of the model complexes have also been performed at the nonlocal DFT level of theory using the exchange functional of Becke[64] and the correlation functional of Perdew[65] (BP86). Scalar relativistic effects have been considered using the ZORA formalism.[66] Uncontracted Slater-type orbitals (STOs) using triple-ζ basis sets augmented by two sets of polarization functions were employed for the SCF calculations.[67] The $(1s)^2$ core electrons of the carbon and oxygen, $(1s2s2p)^{10}$ core electrons of chromium and silicon, $(1s2s2p3s3p3d)^{28}$ core electrons of molybdenum, $(1s2s2p3s3p3d4s4p4d)^{36}$ core electrons of tin, and $(1s2s2p3s3p3d4s4p4d)^{46}$ core electrons of lead and tungsten were treated by the frozen-core

---

(55) Krishnan, R.; Binkley, J. S.; Seeger, R.; Pople, J. A. *J. Chem. Phys.* **1980**, *72*, 650.
(56) McClean, A. D.; Chandler, G. S. *J. Chem. Phys.* **1980**, *72*, 5639.
(57) Hay, P. J.; Wadt, W. R. *J. Chem. Phys.* **1985**, *82*, 299.
(58) Couty, M.; Hall, M. B. *J. Comput. Chem.* **1996**, *17*, 1359.
(59) Ehlers, A. W.; Böhme, M.; Dapprich, S.; Gobbi, A.; Höllwarth, A.; Jonas, V.; Köhler, K. F.; Stegmann, R.; Veldkamp, A.; Frenking, G. *Chem. Phys. Lett.* **1993**, *208*, 111.
(60) Wadt, W. R.; Hay, P. J. *J. Chem. Phys.* **1985**, *82*, 284.
(61) Reed, A. E.; Curtiss, L. A.; Weinhold, F. *Chem. Rev.* **1988**, *88*, 899.
(62) Frisch, M. J.; Trucks, G. W.; Schlegel, H. B.; Scuseria, G. E.; Robb, M. A.; Cheeseman, J. R.; Zarzewski, B. G.; Montgomery, J. A.; Startmann, R. E.; Burant, J. C.; Dapprich, S.; Millam, J. M.; Daniels A. D.; Kudin, K. N.; Straiin, M. C.; Farkas, O.; Tomasi, J.; Barone, V.; Cossi, M.; Cammi, R.; Mennucci, B.; Pomelli, C.; Adamo, C.; Clifford, S.; Ochteriski, J.; Petersson, G. A.; Ayala, P. Y.; Cui, Q.; Morokuma, K.; Salvador, P.; Dannenberg, J. J.; Malick, D. K.; Rabuck, A. D.; Raghavachari, K.; Foresman, J. B.; Cioslowski, J.; Ortiz, J. V.; Baboul A. G.; Stefanov, B. B.; Liu, G.; Liashenko, A.; Piskorz, P.; Komaromi, I.; Gomperts R.; Martin, R. L.; fox, D. J.; Keith, T.; Al-Laham, M. A.; Peng, C. Y.; Nanayakkara, A.; Challacombe, M.; Gill, P. M. W.; Johnson, B. G.; Chen, W.; Wong, M. W.; Andres, J. L.; Gonzalez, C.; Head-Gordon, M.; Replogle, E. S.; Pople, J. A. *Gaussian98*; Gaussian, Inc.: Pittsburgh, PA, 1998.
(63) Schaftenaar, G. *MOLDEN3.4*; CAOSCAMM Center: The Netherlands, 1998.
(64) Becke, A. D. *Phys. Rev. A* **1988**, *38*, 3098.
(65) Perdew, J. P. *Phys. Rev. B* **1986**, *33*, 8822.

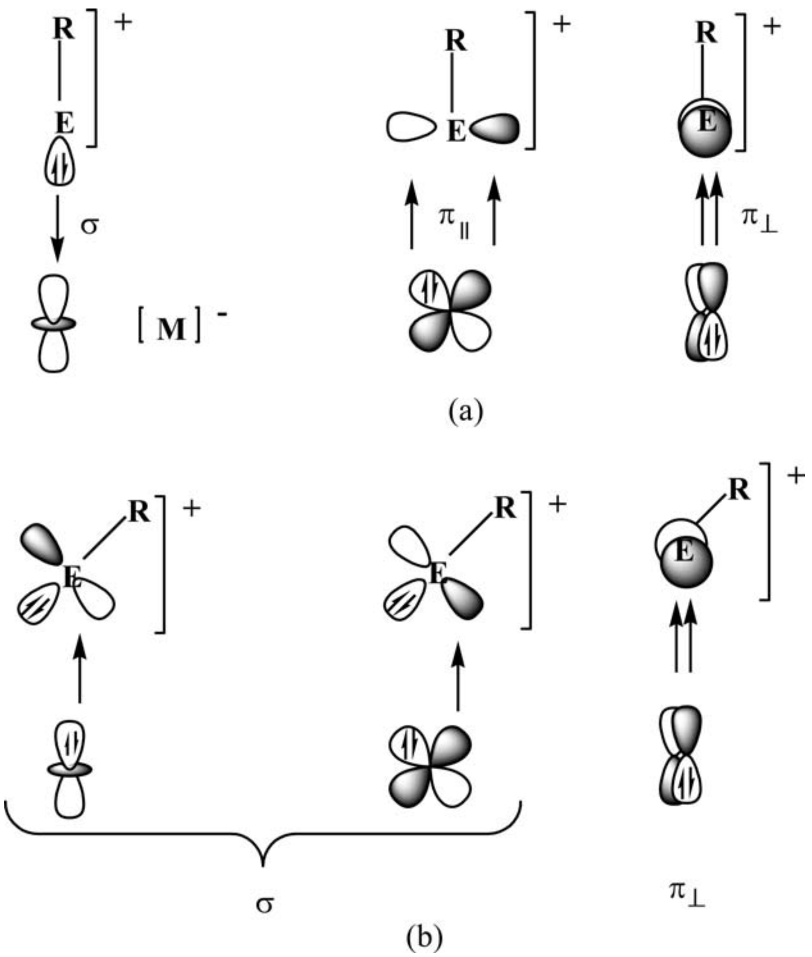

Figure 1. Schematic representation of the orbital interactions between closed-shell metal fragments $[M]^-$ and ligands ER^+ in (a) Metal-ylidyne complexes and (b) Metalloylidenes.

approximation.[68] An auxiliary set of s, p, d, f, and g STOs was used to fit the molecular densities and to present the coulomb and exchange potentials accurately in each SCF cycle.[69] A numerical integration accuracy of INTEGRATION=10 was used throughout. The latter calculations were performed utilizing the program package ADF-2004.01.[70]

The binding interactions between the metal fragments $[(\eta^5\text{-}C_5H_5)(CO)_2M]^-$, $[(\eta^5\text{-}C_5H_5)(CO)_3M]^-$ (M = Cr, Mo, W) and ligands EMe^+ (E = Si, Sn, Pb), as well as the neutral fragments $[(\eta^5\text{-}C_5H_5)(CO)_2M]$, $[(\eta^5\text{-}C_5H_5)(CO)_3M]$ (M = Cr, Mo, W) and ligands EMe, both in their electronic and geometric most stable doublet state, have been analyzed with C_s symmetry using the energy decomposition scheme of ADF which is based on the methods of Morokuma[71] and Ziegler and Rauk.[72] Details of the energy decomposition analysis (EDA) method are given elsewhere[50,52] it has been suggested that the covalent and electrostatic character of a bond is given by the ratio $\Delta E_{\text{elstat}}/\Delta E_{\text{orb}}$.[52,73−75]

Qualitative MO Analysis of the M−(ER) Bond. The geometries, molecular composition, and chemical properties of the molecules suggest that the M−E−R bonding situation in **II** is significantly different from the bonding situation in molecules **I**, featuring triple bonds to ER ligands. A comparison of compounds **II** with **I** shows that the former compounds have one more CO ligand than the latter. Simple molecular orbital arguments give a first explanation about the bonding differences between metal-ylidyne and metallo-ylidene complexes. Electron counting describe

---

(66) (a) Chang, C.; Pelissier, M.; Durand, Ph. *Phys. Scr.* **1986**, *34*, 394. (b) Heully, J.-L.; Lindgren, I.; Lindroth, E.; Lundqvist, S.; Martensson-Pendrill, A.-M. *J. Phys. B* **1986**, *19*, 2799. (c) van Lenthe, E.; Baerends, E. J.; Snijders, J. G. *J. Chem. Phys.* **1993**, *99*, 4597. (d) van Lenthe, E.; Baerends, E. J.; Snijders, J. G. *J. Chem. Phys.* **1996**, *105*, 6505. (e) van Lenthe, E.; van Leeuwen, R.; Baerends, E. J.; Snijders, J. G. *Int. J. Quantum Chem.* **1996**, *57*, 281. (f) van Lenthe, E.; Ehlers, A. E.; Baerends, E. J. *J. Chem. Phys.* **1999**, *110*, 8943.

(67) Snijders, J. G.; Baerends, E. J.; Vernooijs, P. *At. Data Nucl. Data Tables* **1982**, *26*, 483.

(68) Baerends, E. J.; Ellis, D. E.; Ros, P. *Chem. Phys.* **1973**, *2*, 41.

(69) Krijn, J.; Baerends, E. J. *Fit Functions in the HFS-Method*, Internal Report (in Dutch); Vrije Universiteit Amsterdam: The Netherlands, 1984.

(70) Baerends, E. J.; Autschbach, J. A.; Berces, A.; Bo, C.; Boerrigter, P. M.; Cavallo, L.; Chong, D. P.; Deng, L.; Dickson, R. M.; Ellis, D. E.; Fan, L.; Fischer, T. H.; Fonseca Guerra, C.; van Gisbergen, S. J. A.; Groeneveld, J. A.; Gritsenko, O. V.; Grüning, M.; Harris, F. E.; van den Hoek, P.; Jacobsen, H.; van Kessel, G.; Kootstra, F.; van Lenthe, E.; Osinga, V. P.; Patchkovskii, S. Philipsen, P. H. T.; Post, D. Pye, C. C.; Ravenek, W.; Ros, P.; Schipper, P. R. T.; Schreckenbach, G.; Snijders, J. G.; Sola, M.; Swart, M.; Swerhone, D.; te Velde, G.; Vernooijs, P.; Versluis, L.; Visser, O.; Wezenbeek, E.; Wiesenekker, G.; Wolff, S. K.; Woo, T. K.; Ziegler, T. *ADF 2004−01*; Scientific Computing & Modelling NV: The Netherlands.

(71) (a) Morokuma, K. *J. Chem. Phys.* **1971**, *55*, 1236. (b) Morokuma, K. *Acc. Chem. Res.* **1977**, *10*, 294.

(72) (a) Ziegler, T.; Rauk, A. *Theor. Chim. Acta* **1977**, *46*, 1. (b) Ziegler, T.; Rauk, A. *Inorg. Chem.* **1979**, *18*, 1558. (c) Ziegler, T.; Rauk, A. *Inorg. Chem.* **1979**, *18*, 1755.

(73) Diefenbach, A.; Bickelhaupt, M. B.; Frenking, G. *J. Am. Chem. Soc.* **2000**, *122*, 6449.

(74) Uddin, J.; Frenking, G. *J. Am. Chem. Soc.* **2001**, *123*, 1683.

(75) Pandey, K. K. *Inorg. Chem.* **2003**, *42*, 6764.

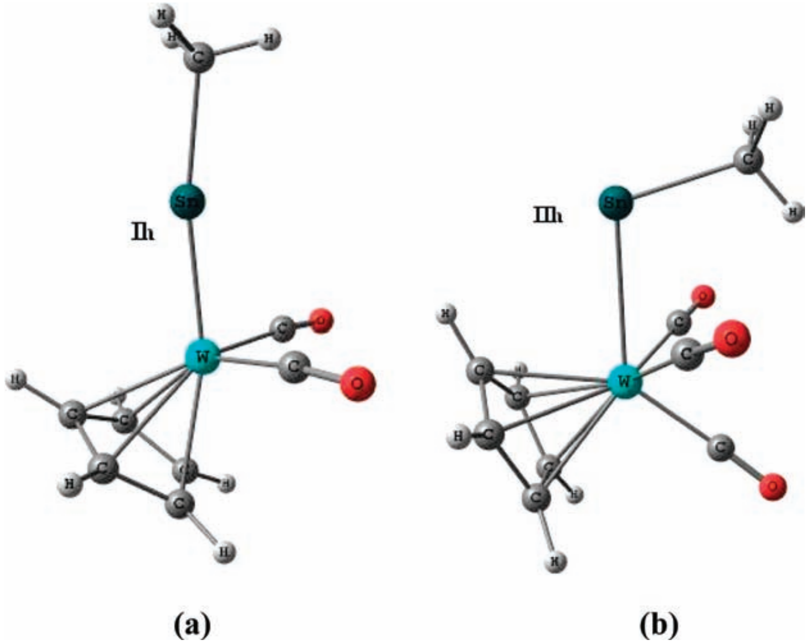

Figure 2. Optimized geometries of the metal-ylidyne complex [(η^5-C_5H_5)(CO)$_2$W≡SnMe] **Ih** (a), and the metallo-ylidene [(η^5-C_5H_5)(CO)$_3$W-SnMe] **IIh** (b). The most important bond lengths and angles are given in Table 1.

[Cp(CO)$_2$M(ER)] molecules as 18-electron species. Adding one CO would lead to 20-electron compounds. To avoid that and keep a 18-electron counting, metal-E bonding must decrease. This is achieved by transforming a bonding pair M−E into a lone pair at E, leading to a bent M−ER geometry in [Cp(CO)$_3$MER] compounds.

The M≡ER bonds in **I** are composed of one σ-bond [$ER^+ \rightarrow d_{z^2}$] and two π-bonds (in-plane $\pi_\perp$) which are schematically shown in Figure 1a. The 18-electron rule suggests that the formally positively charged ligands EMe^+ ligand in **IIa**−**IIi** can not serve as a two electron donor like in **Ia**−**Ii** because the metal fragment of the former species has two more electrons. The d_{z^2} acceptor orbital of the metal is occupied, and thus it cannot serve as a σ acceptor orbital. The other d-orbitals of the metal cannot serve as acceptor orbitals because the interaction is symmetry forbidden. Attractive orbital interactions between ER^+ and the metal fragment of **IIa**−**IIi** are only possible when the ylidyne ligands ER^+ are bonded in a side-on fashion (Figure 1b). The qualitative bonding model in Figure 1b shows that the M−ER bonding has two components, that is, the σ donation from the occupied metal d_{z^2} and d_{yz} orbitals into the in-plane p(π) atomic orbitals (AO) of Si, Ge, Sn and Pb and $\pi_\perp$ donation from the occupied metal d_{xz} orbital into the out-of-plane p(π) atomic orbital of Si, Ge, Sn, and Pb.

This simple picture of the M−(ER) bond will be deepened with the help of DFT calculations, allowing a comparative analysis of the geometries of the complexes and a quantitative analysis of the M−(ER) interaction.

Geometries. Metal-Silylidyne, Metal-Stannylidyne, and Metal-Plumbylidyne Complexes. The optimized geometry of one representative example of the metal-ylidyne complexes (**Ih**) is shown in Figure 2a. Optimized structures of all the complexes of this class (**Ia-Ii**) are given in the Supporting Information. The B3LYP optimized bond lengths and bond angles are presented in Table 1.

There are no structural data for compounds featuring Cr−E triple bonds (E = Si, Sn, Pb). The optimized Mo≡Si bond distance (2.229 Å) in model complex [(η^5-C_5H_5)(CO)$_2$Mo≡SiMe] **IId** is in close agreement with experimental results of [(η^5-C_5Me_5)(depe)(H)Mo≡SiMes][B(C_6H_5)$_4$] (2.219(2) Å).[11] The W≡Sn and M≡Pb bond distances in [(η^5-C_5H_5)(CO)$_2$M≡EMe] (M = W, E = Sn, 2.483 Å; M = Mo, E = Pb, 2.522 Å; M = W, E = Pb, 2.521 Å) are in close agreement with experimental values in [Cl(PMe$_3$)$_4$W(SnAr*)] (2.4901(7) Å),[20] [Br(PMe$_3$)$_4$Mo(PbAr**)] (2.5495(8) Å),[22] [I(PMe$_3$)$_4$W(PbAr**)] (2.5477(3) Å), [Br(PMe$_3$)$_4$W(PbAr**)] (2.5464(5) Å),[23] [H(PMe$_3$)$_4$W(PbAr**)] (2.5525(3) Å),[24] [(PhCN)(PMe$_3$)$_4$W(PbAr**)]$^+$ (2.5520(6) Å) and [PMe$_3$)$_5$W(PbAr**)]$^+$ (2.5744(2) Å).[23] Almost similar values of M≡Sn and M≡Pb bond lengths in the complexes [(η^5-C_5H_5)(CO)$_2$M≡SnMe] and [(η^5-C_5H_5)(CO)$_2$M≡PbMe] (M = Mo, W) are consistent with the similar sizes of molybdenum and tungsten (1.40 Å and 1.41 Å covalent radii for Mo and W).[72] The M≡Sn and M≡Pb bonds are about 0.08 Å longer than the Cr≡Sn and Cr≡Pb bonds, respectively, and this is consistent with the larger sizes of the second and third row elements in comparison to those in first row.

The M≡E bond distances in **Ia**−**Ii** are significantly shorter than those expected from single bonds based on covalent bond predictions (Cr−Si = 2.47 Å, Cr−Sn = 2.69 Å, Cr−Pb = 2.76 Å; Mo−Si = 2.58 Å, Mo−Sn = 2.80 Å, Mo−Pb = 2.87 Å; W−Si = 2.59 Å, W−Sn = 2.81 Å, W−Pb = 2.88 Å).[76] Using the relationship between bond order and bond distances by Pauling, we find that the calculated M−E bond distances correspond to a bond order of ~3.[77]

The E−C optimized bond lengths in complexes **Ia**−**Ii** (Table 1) are slightly shorter than those expected for a single bond based on covalent radii predictions (Si−C = 1.95 Å, Sn−C = 2.17 Å, Pb−C = 2.24 Å). The M−E−C bond angles in complexes **Ia**−**Ii** deviate slightly from linearity.

Metallosilylidene, Metallostannylidene, and Metalloplumbylidene Complexes. Figure 2b shows the optimized geometry of one representative example of the metal-ylidene complexes (**IIh**). Optimized structures of all the complexes of this class (**IIa**−**IIi**) are given in the Supporting Information. The optimized bond lengths and bond angles at B3LYP are presented in Table 1. The metallosilylidenes have not been isolated so far. We report here the structures of these compounds [(η^5-C_5H_5)(CO)$_3$M-SiMe] (M = Cr, Mo, W). The optimized geometries of the model metal-

---

(76) (a) Wells, A. F. *Structural Inorganic Chemistry*, 5th ed.; Clarendon: Oxford, 1984. (b) Pauling, L. *The Nature of the Chemical Bond*, 3rd ed.; Cornell University Press: Ithaca, NY, 1960.

Table 1. Selected Optimized Geometrical Parameters for Metal-ylidyne Complexes $[(Cp)(CO)_2M{\equiv}EMe]$ and Metallo-ylidenes $[(Cp)(CO)_3M{-}EMe]$ (M = Cr, Mo, W; E = Si, Sn, Pb)[a]

	bond distances					bond angles		
	M−E	M−CO	M−C(Cp)	E−C	C−O	M−E−C	E−M−CO	C(O)−M−C(O)
				Metal-ylidyne Complexes				
$[(Cp)(CO)_2Cr{\equiv}SiMe]$	2.128	1.763	2.103	1.854	1.173	173.9	83.5	90.7
$[(Cp)(CO)_2Cr{\equiv}SnMe]$	2.399	1.758	2.093	2.122	1.175	172.6	85.3	94.8
$[(Cp)(CO)_2Cr{\equiv}PbMe]$	2.438	1.756	2.089	2.176	1.756	171.7	84.7	93.0
$[(Cp)(CO)_2Mo{\equiv}SiMe]$.	2.229	1.978	2.404	1.887	1.156	168.0	87.3	90.1
$[(Cp)(CO)_2Mo{\equiv}SnMe]$	2.482	1.975	2.389	2.159	1.158	163.6	87.1	90.3
$[(Cp)(CO)_2Mo{\equiv}PbMe]$	2.522	1.974	2.387	2.232	1.158	1.648	87.6	90.2
$[(Cp)(CO)_2W{\equiv}SiMe]$	2.239	1.973	2.386	1.884	1.159	173.3	88.5	90.4
$[(Cp)(CO)_2W{\equiv}SnMe]$	2.483	1.969	2.372	2.152	1.161	169.6	88.4	90.5
$[(Cp)(CO)_2W{\equiv}PbMe]$	2.521	1.968	2.369	2.220	1.162	170.9	88.8	90.5
				Metallo-ylidenes				
$[(Cp)(CO)_3Cr\text{-}SiMe]$	2.482	1.771 (1.770)	2.167	1.909	1.172 (1.165)	106.4	69.1 (122.8)	109.4
$[(Cp)(CO)_3Cr\text{-}SnMe]$	2.811	1.850 (1.849)	2.244	2.192	1.159 (1.149)	103.8	67.9 (126.7)	110.3
$[(Cp)(CO)_3Cr\text{-}PbMe]$	2.918	1.850 (1.847)	2.252	2.269	1.160 (1.150)	102.4	67.3 (126.7)	109.7
$[(Cp)(CO)_3Mo\text{-}SiMe]$	2.626	1.986 (1.997)	2.421	1.914	1.156 (1.148)	112.4	69.2 (129.2)	103.2
$[(Cp)(CO)_3Mo\text{-}SnMe]$	2.909	1.986 (1.992)	2.411	2.190	1.159 (1.149)	105.5	68.3 (128.2)	103.7
$[(Cp)(CO)_3Mo\text{-}PbMe]$	3.015	1.985 (1.988)	2.410	2.270	1.160 (1.151)	104.0	67.7 (128.0)	103.6
$[(Cp)(CO)_3W\text{-}SiMe]$	2.628	1.978 (1.989)	2.405	1.913	1.160 (1.152)	112.1	69.4 (129.1)	102.9
$[(Cp)(CO)_3W\text{-}SnMe]$	2.918	1.978 (1.983)	2.395	2.189	1.162 (1.153)	105.3	68.5 (128.0)	103.8
$[(Cp)(CO)_3W\text{-}PbMe]$	3.025	1.976 (1.979)	2.393	2.268	1.164 (1.154)	103.6	67.7 (127.9)	103.7

[a] Distances are in Å and angles are in degrees.

lostannylidenes, $[(\eta^5\text{-}C_5H_5)(CO)_3M\text{-}SnMe]$ and metalloplumbylidenes, $[(\eta^5\text{-}C_5H_5)(CO)_3M\text{-}PbMe]$ are in good agreement with experimental results of $[(\eta^5\text{-}C_5H_5)(CO)_3M{-}ER]$[26,27] (Chart 2). The bent geometries at silicon, tin, and lead (M−E−C bond angles in the range 102.4°−112.4°) in these compounds are consistent with the presence of a divalent Si(II), Sn(II), and Pb(II) center, which is singly bonded to a transition metal and carbon. The M−E bond lengths (Cr−Si = 2.482 Å, Mo−Si = 2.626 Å, W−Si = 2.628 Å; Cr−Sn = 2.811 Å, Mo−Sn = 2.909 Å, W−Sn = 2.918 Å; Cr−Pb = 2.918 Å, Mo−Pb = 3.015 Å, W−Pb = 3.025 Å) are longer than those expected for a single bond based on covalent radii predictions (Cr−Si = 2.47 Å, Cr−Sn = 2.69 Å, Cr−Pb = 2.76 Å; Mo−Si = 2.58 Å, Mo−Sn = 2.80 Å, Mo−Pb = 2.87 Å; W−Si = 2.59 Å, W−Sn = 2.81 Å, W−Pb = 2.88 Å).[76] On going from metallosilylidenes to metalloplumbylidenes we note a steady increase in the M−E bond length.

The optimized Si−C, Sn−C, and Pb−C bond distances in **IIa**−**IIi** are longer than those found in the complexes **Ia**−**Ii** (Table 1) and approximately similar to a single bond based on covalent radii predictions (Si−C = 1.95 Å, Sn−C = 2.17 Å, Pb−C = 2.24 Å). The Sn−C and Pb−C bond lengths and M−E−C bond angles in metallostannylidenes and metalloplumbylidenes are within the range of mononuclear stannylidenes and plumbylidenes.[49] Hence, the calculated geometries of the compounds **IIa**−**IIi** agree with those of the known structures of stannylidenes and plumbylidenes with one metal fragment as a substituent.

Bonding Analysis of M≡EMe and M−EMe Bonds. To get detailed insight into the nature of the M−ER interactions, we carried out an energy decomposition analysis. The charges on the ER ligands are significantly positive, with values ranging from +0.63 to +0.81 in metal-ylidyne complexes and from +0.35 to +0.53 in metallo-ylidenes (see above). For this reason we have considered $[M]^-$ and $[ER]^+$ fragments in the decomposition analysis. However, to assess the dependence of our results with the charge on the fragments and be able to compare the computed BDEs with the previous ones reported in the literature, we have also considered the homolytic dissociation into the neutral [M] and [ER] fragments.

Table 2 shows homolytic bond dissociation energies of M≡E and M−E bonds. The dissociation energies of multiple bonds of other ylidyne complexes reported in the literature[15,18,21−23,51] are also collected in Table 2. Our values are in the same range than those reported with the same metal ligands. Comparing complexes with the same metal and the same E, M−E binding energies are considerably lower (between 19−45% lower) than M≡E BDEs. The magnitude of the energy terms slightly decreases in the order W > Mo > Cr as coordinating metal. From periodic trends the chromium complexes are expected to have the weakest M≡E and M−E bonds. However, as is seen, even the Cr≡E bonds and Cr−E bonds are predicted to be quite strong. The tabulated results for W reveal the expected periodic trend in bond strengths due to d-orbital extent: the W≡E and W−E bonds are slightly stronger than corresponding Mo≡E and Mo−E bonds. Binding energies become considerably small as E becomes heavier: on going from silylidyne to plumbylidyne complexes, we note a steady decrease in the bond dissociation energies. A remarkable influence of the charge on the ligand set can be appreciated comparing BDEs of plumbylidyne complexes. The reported dissociation energy of the $[Pb(2,6\text{-}Trip_2C_6H_3)]^+$ cation in the plumbylidyne complex with a neutral set of ligands ($[(PMe_3)_5W{\equiv}Pb(2,6\text{-}Trip_2C_6H_3)]^+$, BDE = 35.8 kcal/mol)[23] is about a half of those calculated with a negative charge on the ligands set ($L_n = Cp(CO)_2$).

According to the charges in the fragments, the energy decomposition analysis has been initially performed considering $[M]^-$ and

Table 2. Homolytic BDEs of the M−E Bond in Metal-ylidyne and Metallo-ylidene Complexes (kcal/mol)

E	L_n	R	BDE(M≡E)	BDE(M−E)[a]	ref
			M = Cr		
Si	$Cp(CO)_2$	H	68.1		51
Si	$Cp(CO)_2$	Me	75.7	50.7	this work
Ge	$Cp(CO)_2$	H	58.5		51
Ge	$Cp(CO)_2$	Me	76.2 (60.8)[b]	47.0	this work
Ge	$Cp(CO)_2$	Ph	57.6		51
Ge	$Cp(CO)_2$	Ar[c]	55.1		51
Sn	$Cp(CO)_2$	H	46.7		51
Sn	$Cp(CO)_2$	Me	63.8	44.0	this work
Pb	$Cp(CO)_2$	H	41.5		51
Pb	$Cp(CO)_2$	Me	51.3	41.4	this work
Pb	$Cp(CO)_2$	Ar[c]	41.1		51
			M = Mo		
Si	$Cp(CO)_2$	H	85.9		51
Si	$Cp(CO)_2$	Me	87.8	54.0	this work
Ge	$Cp(CO)_2$	H	76.3		51
Ge	$Cp(CO)_2$	Me	83.2	52.6	this work
Sn	$Cp(CO)_2$	H	64.8		51
Sn	$Cp(CO)_2$	Me	71.3	49.7	this work
Pb	$Cp(CO)_2$	H	58.8		51
Pb	$Cp(CO)_2$	Me	64.0	47.2	this work
Pb	$Cp(CO)_2$	Ar[c]	57.2		51
Pb	$Br(PH_3)_4$	Ar[c]	46.7		22
			M = W		
Si	$Cp(CO)_2$	H	99.9		51
Si	$Cp(CO)_2$	Me	100.1	56.4	this work
Ge	$Cp(CO)_2$	H	89.3		51
Ge	$Cp(CO)_2$	Me	96.2	54.7	this work
Ge	$Cl(CO)_4$	Cp	65.4		15
Ge	$Cl(PH_3)_4$	Cp	54.8		15
Ge	$Cl(PH_3)_4$	Me	84.9		18
Sn	$Cp(CO)_2$	H	75.9		51
Sn	$Cp(CO)_2$	Me	81.7	50.8	this work
Sn	$Cl(PH_3)_4$	Me	70.6		21
Pb	$Cp(CO)_2$	H	69.0		51
Pb	$Cp(CO)_2$	Me	72.1	48.0	this work
Pb	$Cp(CO)_2$	Ar[c]	67.3		51
Pb	$(PMe_3)_5$	Ar[c]	35.8		23

[a] $L_n = Cp(CO)_3$. [b] ref 51. [c] Ar = C_6H_3-2,6(C_6H_2-2,4,6-*i*Pr_3)$_2$.

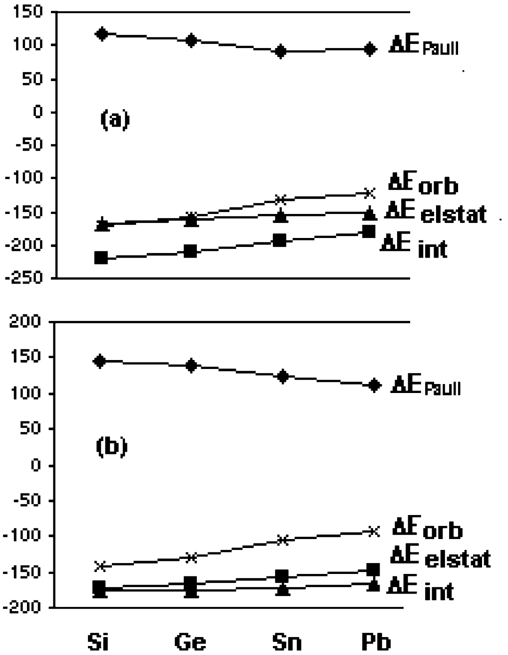

Figure 3. Trends of the different energy terms of the EDA (in kcal/mol) from silicon to lead in the [(η^5-C_5H_5)$(CO)_2$M≡EMe] (above) and [(η^5-C_5H_5)$(CO)_3$M−EMe] complexes (below). $[M]^-$ and $[ER]^+$ fragments have been considered.

$[ER]^+$ fragments. The trends of the different energy terms arising from the EDA from silicon to lead in the [(η^5-C_5H_5)$(CO)_2$M≡EMe] and [(η^5-C_5H_5)$(CO)_3$M−EMe] complexes are shown in Figure 3, and the energy terms collected in Tables 3 and 4.

The calculated data in Table 3 shows that the interaction energies of the linear M≡EMe complexes **Ia**−**Ii** (−162.8 to −231.0 kcal/mol) are rather high. On going from silicon to lead, the interaction energies decrease (Figure 3). The contributions of the electrostatic interactions, $\Delta E_{\mathrm{elstat}}$, and the covalent bonding, ΔE_{orb}, have nearly the same values for silylidyne and germylidyne complexes, while for the stannylidyne and plumbylidyne complexes, the electrostatic interactions, $\Delta E_{\mathrm{elstat}}$, are greater than the orbital interaction, ΔE_{orb}. The σ-bonding in [(η^5-C_5H_5)$(CO)_2$M≡EMe] (M = Cr, Mo, W; E = Si, Ge, Sn, Pb) has lower degree of covalent character (42.1−50.2). The covalent bonding has a high degree of π-character. We want to emphasize that the calculated energy contribution ΔE_π in the complexes **Ia**−**Ii** gives only the out of plane ($\pi_\perp$) component of the total $[M]^-$−$[EMe]^+$ π back-donation, which is schematically shown in Figure 1a. This is because the molecules have C_s symmetry, and thus, the molecular orbitals can only have a′ (σ) or a″ (π) symmetry. Thus, the energy contributions of the a′ (σ) molecular orbitals come from the $[M]^- \rightarrow EMe^+$ σ-donation but also from the in-plane $[M]^- \rightarrow EMe^+$ π back-donation. For molecules which have only C_s symmetry, it is not possible to separate the latter two interactions because the molecular orbitals have a′ symmetry. An energy partitioning analysis of the germylidyne complex [$Cl(CO)_4$W≡GeH],[50] the stannylidyne complex [$Cl(PH_3)_4$W≡SnMe],[21] and plumbylidyne complex [$Br(PH_3)_4$-Mo≡PbPh][22] have shown that the total contribution of π back-donation is 78.0%, 81.0%, and 82.9% of ΔE_{orb}, respectively.

The energy analysis suggests that in [(η^5-C_5H_5)$(CO)_2$M≡EMe] (M = Cr, Mo, W; E = Si, Ge, Sn, Pb) complexes, ~42% of the ΔE_{orb} comes from (a″) π bonding. On going from silylidyne to plumbylidyne complexes, we note a steady decrease in interaction energy, ΔE_{int}, and orbital interactions, ΔE_{orb}. The most drastic change in covalent bonding, ΔE_{orb}, is observed between germylidyne and stannylidyne complexes (Table 3). The magnitude of the energy terms slightly decreases in the order Cr > Mo > W as coordinating metal.

Let us analyze the differences between the energy contributions to the M≡EMe and M−EMe bonding. First, the total interaction energy ΔE_{int} in the compound **IIa**−**IIi** are less attractive than those in the complexes **Ia**−**Ii**. The M−ER bonds have a slightly lower degree of covalent bonding (34.9−44.9%) than the M≡EMe bonds (42.1−50.2%) (Table 4). However, the drastic difference between the two classes of compounds are found for the degree of a″ (π) bonding. The contribution of ΔE_π to the covalent term ΔE_{orb} is much higher in the M≡EMe bonding (41.6−42.6%) than in the M−EMe bonding (17.1−20.4%). This shows that the a″ (π) contributions to the $[M]^-$−EMe^+ bonding in the compounds **IIa**−**IIi** are much weaker than the out-of-plane π contributions in the complexes **Ia**−**Ii**. This can be explained with the much longer M−E bond lengths in the compounds **IIa**−**IIi** than in the complexes **Ia**−**Ii**. Another factor which contributes to the weaker a″ (π) bonding in **IIa**−**IIi** is that the $[M]^- \rightarrow [EMe]^+$ π back-donation competes with the π-acceptor strength of the three CO ligands, while there are only two CO ligands in **Ia**−**Ii.** While the π bonding contributions in **IIa**−**IIi** are weaker than those in **Ia**−**Ii**, the σ-bonding contributions in the former compounds are stronger than those in the latter. It is significant to note that not only the relative (%) values, but also the absolute values of ΔE_σ in **IIa**−**IIi** are larger than those in **Ia**−**Ii** (Table 3 and Table 4).

Table 3. Energy Decomposition Analysis[a] of Metal-ylidyne Complexes [(Cp)(CO)$_2$M≡EMe] (M = Cr, Mo, W; E = Si, Ge[b], Sn, Pb) at BP86/TZ2P Level[c]

M=	Cr				Mo				W			
E=	Si	Ge	Sn	Pb	Si	Ge	Sn	Pb	Si	Ge	Sn	Pb
ΔE_{int}	−203.1	−206.2	−175.2	−162.8	−220.9	−210.5	−193.6	−180.3	−231.0	−220.6	−202.0	−187.9
ΔE_{Pauli}	135.8	107.9	98.3	102.4	117.0	107.7	90.7	92.7	129.8	115.9	100.8	104.9
ΔE_{elstat}	−173.9	−157.8	−150.8	−153.4	−168.1	−160.8	−153.5	−153.0	−180.7	−168.9	−162.8	−163.8
$\Delta E_{\text{orb}}{}^{d}$	−165.0	−156.3	−122.7	−111.7	−169.7	−157.4	−130.8	−120.0	−180.1	−167.5	−140.0	−129.1
	(48.7%)	(49.8%)	(44.7%)	(42.1%)	(50.2%)	(49.5%)	(46.0%)	(44.0%)	(49,9%)	(49.8%)	(46.2%)	(44.1%)
$\Delta E_{\sigma}(a')$	−96.6	−89.7	−71.0	−64.2	−98.4	−90.7	−75.6	−69.1	−105.2	−97.0	−81.7	−75.2
$\Delta E_{\pi}(a'')^{e}$	−68.4	−66.6	−51.7	−47.5	−71.7	−66.7	−55.2	−50.9	−74.9	−70.5	−58.3	−53.8
	(41.6%)	(42.6%)	(42.1%)	(42.5%)	(42.3%)	(42.4%)	(42.2%)	(42.4%)	(41.6%)	(42.1%)	(41.6%)	(41.7%)
ΔE_{prep}	12.8	5.2	14.1	14.5	9.9	5.8	7.9	7.4	10.9	7.4	8.7	8.0
ΔE ($-D_e$)	−190.3	−201.0	−161.1	−148.3	−211.0	−204.7	−185.7	−172.9	−220.1	−213.2	−193.3	−179.9

[a] Energy contributions in kcal/mol. [b] Energy data are taken from ref 52. [c] [M]$^-$and [ER]$^+$ fragments have been considered (see text). [d] The values in parentheses are the percentage contribution to the total attractive interactions reflecting the covalent character of the bond. [e] The values in parentheses are the percentage contribution in the total orbital interactions, ΔE_{orb}.

Table 4. Energy Decomposition Analysis[a] of Metallo-ylidenes [(Cp)(CO)$_3$M−EMe] (M = Cr, Mo, W; E = Si, Ge[b], Sn, Pb) at BP86/TZ2P Level[c]

M=	Cr				Mo				W			
E=	Si	Ge	Sn	Pb	Si	Ge	Sn	Pb	Si	Ge	Sn	Pb
ΔE_{int}	−169.2	−165.1	−156.1	−146.7	−172.2	−165.6	−156.0	−146.6	−174.8	−168.1	−157.9	−148.1
ΔE_{Pauli}	168.7	138.2	126.5	113.6	145.8	137.5	123.7	111.1	155.9	147.2	128.9	114.7
ΔE_{elstat}	−192.0	−178.2	−177.7	−169.6	−174.9	−174.7	−173.0	−165.5	−182.2	−181.9	−177.9	−169.2
$\Delta E_{\text{orb}}{}^{d}$	−145.9	−125.2	−104.9	−90.8	−143.1	−128.5	−106.8	−92.3	−148.6	−133.4	−108.8	−93.6
	(43.2%)	(41.3%)	(37.1%)	(34.9%)	(45.0%)	(42.4%)	(38.2%)	(35.8%)	(44.9%)	(42.3%)	(38.0%)	(35.6%)
$\Delta E_{\sigma}(a')$	−116.7	−99.6	−84.8	−73.8	−114.8	−103.6	−87.5	−76.2	−119.7	−107.7	−89.5	−77.6
$\Delta E_{\pi}(a'')^{e}$	−29.2	−25.6	−20.1	−17.0	−28.3	−24.9	−19.3	−16.1	−28.9	−25.7	−19.3	−16.0
	(20.0%)	(20.4%)	(19.2%)	(18.7%)	(19.8%)	(19.4%)	(18.1%)	(17.4%)	(19.4%)	(19.3%)	(17.7%)	(17.1%)
ΔE_{prep}	25.8	13.5	14.8	13.2	15.9	12.3	13.9	11.2	14.6	12.4	12.5	10.9
ΔE ($-D_e$)	−143.4	−151.6	−141.1	−133.5	−156.3	−153.3	−142.1	−135.4	−160.2	−155.7	−145.4	−137.2

[a] Energy contributions in kcal/mol. [b] Energy data are taken from ref 52. [c] [M]$^-$ and [ER]$^+$ fragments have been considered (see text). [d] The values in parentheses are the percentage contribution to the total attractive interactions reflecting the covalent character of the bond. [e] The values in parentheses are the percentage contribution in the total orbital interactions, ΔE_{orb}.

Table 5. Energy Decomposition Analysis[a] of Metal-ylidyne Complexes [(Cp)(CO)$_2$M≡EMe] (M = Cr, Mo, W; E = Si, Ge, Sn, Pb) at BP86/TZ2P Level Using Neutral Fragments[b]

M=	Cr				Mo				W			
E=	Si	Ge	Sn	Pb	Si	Ge	Sn	Pb	Si	Ge	Sn	Pb
ΔE_{int}	−95.4	−93.5	−80.9	−70.9	−105.3	−98.4	−86.7	−79.3	−118.2	−111.7	−97.5	−89.0
ΔE_{Pauli}	200.5	159.2	120.3	140.8	184.8	167.5	137.8	133.3	203.2	182.5	152.4	149.4
ΔE_{elstat}	−123.3	−97.1	−76.3	−88.0	−121.1	−108.5	−92.4	−87.4	−138.6	−123.1	−105.0	−100.7
$\Delta E_{\text{orb}}{}^{c}$	−172.6	−155.6	−124.9	−123.8	−169.1	−157.4	−132.2	−125.1	−182.9	−171.1	−145.0	−137.6
	(58.3%)	(61.6%)	(62.1%)	(58.5%)	(58.3%)	(59.2%)	(58.9%)	(58.9%)	(56.9%)	(58.2%)	(58.0%)	(57.4%)
$\Delta E_{\sigma}(a')$	−82.3	−71.8	−56.7	−53.4	−80.7	−83.8	−60.8	−54.4	−89.8	−82.7	−69.5	−62.5
$\Delta E_{\pi}(a'')^{d}$	−90.3	−83.8	−68.2	−70.4	−88.4	−98.4	−71.4	−70.7	−93.1	−88.4	−75.5	−75.1
	(52.3%)	(53.8%)	(54.6%)	(56.9%)	(52.3%)	(54.0%)	(54.0%)	(56.5%)	(50.9%)	(51.7%)	(52.1%)	(54.6%)
$\Delta E_{\text{prep}}{}^{e}$	19.7	17.3	17.1	19.6	17.5	15.2	15.4	15.3	18.1	15.5	15.8	16.6
ΔE ($-D_e$)	−75.7	−76.2	−63.8	−51.3	−87.8	−83.2	−71.3	−64.0	−100.1	−96.2	−81.7	−72.1

[a] Energy contributions in kcal/mol. [b] [(Cp)(CO)$_2$M]and [EMe] in the doublet state. [c] The values in parentheses are the percentage contribution to the total attractive interactions reflecting the covalent character of the bond. [d] The values in parentheses are the percentage contribution in the total orbital interactions, ΔE_{orb}. [e] Preparation energy including unrestricted corrections.

The EDA results of the interaction between neutral fragments [(Cp)(CO)$_2$M], [(Cp)(CO)$_3$M], and ligands [EMe$_3$] (M = Cr, Mo, W; E = Si, Ge, Sn, Pb) are given in Table 5 and Table 6. Table 5 shows that, for the interactions between neutral fragments in metal-ylidyne complexes, the contribution of the π-electrons to the ΔE_{orb} term are larger than the σ contributions. Values of the Pauli repulsive terms, ΔE_{Pauli} are significantly larger for interactions between neutral fragments than for interactions between charged fragments (Table 3). For metallo-ylidenes (Table 6), the interactions between neutral fragments show a strong σ bond and very weak π bond between the fragments. The orbital interactions ΔE_{orb} are larger than the electrostatic interactions ΔE_{elstat}.

Table 7 gives the Wiberg bond indices (WBI).[78] The natural bond orbital (NBO) charge distributions are presented in Figure 4 and Figure 5. Table 7 shows that the WBI values of the M≡E bonds in the complexes having linear M≡E−R linkage, **Ia**−**Ii** are significantly higher (1.23−1.64) than the WBI values of the M−E bonds in the compounds having bent M−E−R linkage, **IIa**−**IIi** (0.32−0.74). The latter values are approximately one-third of the WBI values of the M≡E bonds. This is a first hint that the complexes **Ia**−**Ii** have a substantial degree of multiple M−E bonding. The bond indices of the E−CH$_3$ and M-CO bonds of the two classes of compounds are not very different from each other. The calculated charge distribution indicates that the silicon, germanium,[52] tin and lead atoms and EMe ligands are positively charged in the two classes of complexes. The EMe ligands in the

---

(77) Pauling L. *The Nature of the Chemical Bond*, 3rd ed.; Cornell University Press: New York, 1960; p 239; the relationship of bond order to length is given by $d_n = d_1 - 0.71 \log(n)$ where n is the bond order, d_1 and d_n are the lengths of bonds with bond order 1 and n, respectively.

(78) Wiberg, K. A. *Tetrahedron* **1968**, *24*, 1083.

Table 6. Energy Decomposition Analysis[a] of Metallo-ylidenes [(Cp)(CO)$_3$M−EMe] (M = Cr, Mo, W; E = Si, Ge[b], Sn, Pb) at BP86/TZ2P Level Using Neutral Fragments[c]

M=	Cr				Mo				W			
E=	Si	Ge	Sn	Pb	Si	Ge	Sn	Pb	Si	Ge	Sn	Pb
ΔE_{int}	−67.0	−63.1	−59.2	−56.4	−68.4	−65.6	−62.2	−59.4	−71.6	−68.1	−63.9	−60.7
ΔE_{Pauli}	193.3	214.0	216.2	193.7	227.2	217.9	193.5	173.8	263.9	242.4	218.8	195.0
ΔE_{elstat}	−136.9	−101.9	−104.8	−94.5	−121.5	−117.7	−105.5	−94.9	−136.3	−127.0	−115.8	−103.4
ΔE_{orb}[b]	−223.4	−175.2	−170.6	−155.6	−174.1	−165.8	−150.2	−138.3	−198.6	−183.5	−166.8	−152.3
	(62.0%)	(63.2%)	(61.9%)	(62.2%)	(58.9%)	(58.5%)	(58.7%)	(59.3%)	(59.3%)	(59.1%)	(59.0%)	(59.6%)
$\Delta E_{\sigma}(a')$	−208.8	−164.1	−161.2	−148.4	−160.2	−153.7	−141.4	−131.7	−184.7	−171.8	−158.4	−146.0
$\Delta E_{\pi}(a'')$[d]	−14.6	−11.1	−9.4	−7.1	−13.9	−12.1	−8.8	−6.6	−13.9	−11.7	−8.4	−6.3
	(6.5%)	(6.3%)	(5.5%)	(4.6%)	(8.3%)	(7.3%)	(5.8%)	(4.8%)	(7.0%)	(6.4%)	(5.0%)	(4.1%)
ΔE_{prep}[e]	17.3	16.1	15.2	15.0	14.4	13.0	12.5	12.2	15.2	13.4	13.1	12.7
ΔE ($-D_e$)	−50.7	−47.0	−44.0	−41.4	−54.0	−52.6	−49.7	−47.2	−56.4	−54.7	−50.8	−48.0

[a] Energy contributions in kcal/mol. [b] The values in parentheses are the percentage contribution to the total attractive interactions reflecting the covalent character of the bond. [c] [(Cp)(CO)$_3$M]and [EMe] in the doublet state. [d] The values in parentheses are the percentage contribution in the total orbital interactions, ΔE_{orb}. [e] Preparation energy including unrestricted corrections.

Table 7. Wiberg Bond Indices (WBI), and Results of the NBO Analysis in Metal-ylidyne Complexes [(Cp)(CO)$_2$Mo≡EMe] and Metallo-ylidenes [(Cp)(CO)$_3$Mo-EMe] (E = Si, Sn, Pb)

	metal-ylidyne complexes									metallo-ylidenes								
	Cr			Mo			W			Cr			Mo			W		
	Si	Sn	Pb	Si	Sn	Pb	Si	Sn	Pb	Si	Sn	Pb	Si	Sn	Pb	Si	Sn	Pb
	Wiberg Bond Indices																	
M−E	1.33	1.17	1.05	1.54	1.34	1.23	1.64	1.43	1.31	0.37	0.32	0.32	0.54	0.39	0.36	0.55	0.40	0.37
M−CO	1.02	1.04	1.05	1.07	1.09	1.10	1.13	1.16	1.17	0.97	0.96	0.98	1.04	1.07	1.08	1.10	1.13	1.14
										(0.92)	(0.90)	(0.93)	(0.97)	(0.98)	(1.00)	(1.01)	(1.04)	(1.05)
E−CH3	0.78	0.60	0.56	0.82	0.66	0.65	0.84	0.69	0.67	0.77	0.65	0.68	0.78	0.66	0.69	0.78	0.66	0.70
C−O	2.00	1.99	1.99	2.05	2.02	2.02	2.01	1.98	1.98	2.02	2.04	2.02	2.03	2.01	2.01	2.00	1.98	1.97
										(2.08)	(2.12)	(2.11)	(2.11)	(2.11)	(2.10)	(2.08)	(2.07)	(2.06)
	NBO Analysis																	
M−E σ-bond occupancy	1.892	1.817	1.780	1.888	1.809	1.581	1.907	1.834	1.945	1.658	1.473	1.485	1.634	1.584	1.579	1.602	1.549	1.971
M																		
%	46.35	48.64	44.87	39.80	38.16		39.87	40.77	30.00	47.84	82.03	81.84	76.54	84.34	85.08	73.85	81.73	
%s	36.06	32.99	31.08	33.61	36.09		35.40	37.54	39.20	7.55	13.10	10.59	5.38	3.24	2.22	7.54	5.37	
%p	0.06	0.09	0.12	0.09	0.16		0.12	0.29	0.21	0.06	0.01	0.02	0.18	0.15	0.10	0.31	0.25	
%d	63.87	66.92	68.80	66.28	63.74		64.45	62.15	60.58	92.39	86.78	89.39	94.44	96.61	97.68	92.15	94.38	
E						LP(Pb)[a]												LP(Pb)
%	53.65	51.36	55.13	60.20	61.84	100.00	60.13	59.23	70.00	52.16	17.97	18.16	23.46	15.66	14.92	26.15	18.27	100.00
%s	52.73	52.40	44.58	55.22	54.01	91.00	55.85	53.72	85.88	53.51	4.62	2.67	8.64	6.63	4.31	9.41	6.75	90.49
%p	47.25	47.56	55.30	44.76	45.99	09.00	44.12	46.26	14.08	46.44	95.26	97.28	90.94	93.31	95.67	90.11	93.17	9.51
%d	0.02	0.04	0.12	0.03	0.01	0.00	0.04	0.01	0.04	0.05	0.12	0.05	0.42	0.05	0.01	0.48	0.08	0.00
E−CH$_3$ bond occupancy	1.988	1.956	1.926	1.982	1.958	1.870	1.984	1.958		1.931	1.978	1.978	1.975	1.976	1.978	1.973	1.974	1.976
E																		
%	32.20	29.07	32.16	28.88	25.16	21.99	29.38	26.04		33.99	19.98	21.24	24.52	20.14	21.74	24.86	20.36	22.27
%s	43.90	45.56	44.58	38.74	39.47	9.13	38.07	39.67		45.67	9.54	6.23	13.90	9.75	6.55	14.51	9.94	7.16
%p	55.70	54.31	55.30	60.82	60.48	90.86	61.52	60.28		53.94	90.43	93.74	85.28	90.22	93.43	84.69	90.03	92.82
%d	0.40	0.13	0.11	0.44	0.05	0.01	0.41	0.05		0.38	0.04	0.03	0.82	0.03	0.02	0.80	0.03	0.02
C(CH$_3$)																		
%	67.80	70.93	67.84	71.12	74.84	78.01	70.62	73.96		66.01	80.02	78.76	75.48	79.86	78.26	75.14	79.64	77.73
%s	26.66	21.82	19.48	27.34	23.06	21.80	27.53	23.01		23.56	26.12	23.16	29.51	25.74	23.03	29.48	25.70	22.94
%p	73.18	70.10	80.45	72.51	76.87	78.16	72.32	76.92		76.30	73.84	76.81	70.34	74.21	76.95	70.38	74.26	77.04
%d	0.16	0.08	0.07	0.15	0.07	0.04	0.15	0.07		0.13	0.04	0.02	0.15	0.04	0.02	0.14	0.04	0.02

[a] LP(Pb) = Lone-pair on lead.

complexes **Ia−Ii** are more positively charged than that in compounds **IIa−IIi**. Considering [(η^5-C_5H_5)(CO)$_n$M]$^-$ and [EMe]$^+$ as interacting fragments, we note that there is an over all charge flow in the direction [(η^5-C_5H_5)(CO)$_n$M]$^-$ → [EMe]$^+$, although the charge flow in **IIa−IIi** is larger than in **Ia−Ii** (Figure 4 and Figure 5).

A more definitive picture of the M≡ER and M−E−R bonding is obtained through a NBO analysis of the delocalized Kohn−Sham orbitals. The characteristic of the M≡EMe, and E−CH$_3$ orbitals are listed in Table 7. In the M≡EMe bond, the M−E σ-bonding orbitals are always polarized toward the silicon, tin and lead atoms, and the polarization increases from chromium to tungsten. In contrast, in the M−EMe bond, the M−E σ-bonding orbitals are significantly polarized toward the metal atom. The occupations for M−E−R σ-bonding orbitals are relatively smaller. In the E−CH$_3$ bond, the E−C σ-bonding orbitals are polarized toward the C atom in both types of complexes. The hybridization of the E−CH$_3$ σ-bonds at the silicon, tin and lead atom has greater s-character in **Ia−Ii** than those in **IIa−IIi**. This is one of the reasons for shortest E−CH$_3$ bond in the **Ia−Ii**. The difference in the σ (a′) interactions for compounds **I** and **II** may be explained with the different hybridization of the M≡E and M−E σ bonds at the metal center and E atoms (Table 5). The hybridization at the metal atoms in the M≡E bonds has d character in the range 60.6−68.8%, while the M−E bonds has large d character which is always >86% of the total AO contribution. The hybridization of the M≡E bond at the group 14-elements has relatively lesser p-character about 45% (except 14.08% in **Ii**), while the M−E bond has a large p-character which is >90% (except **IIa**) of the total AO contribution. The trend

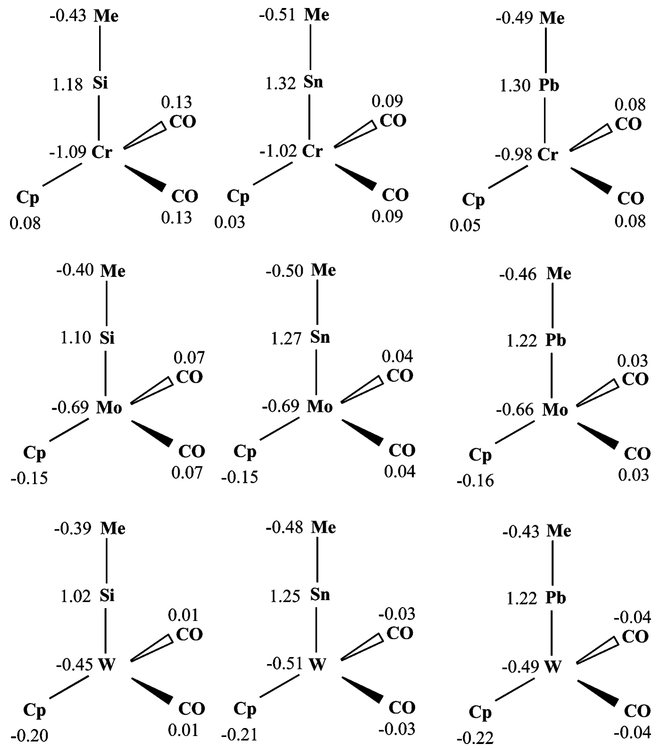

Figure 4. Calculated NBO partial charges of the metal-ylidyne complexes **Ia**−**Ii**.

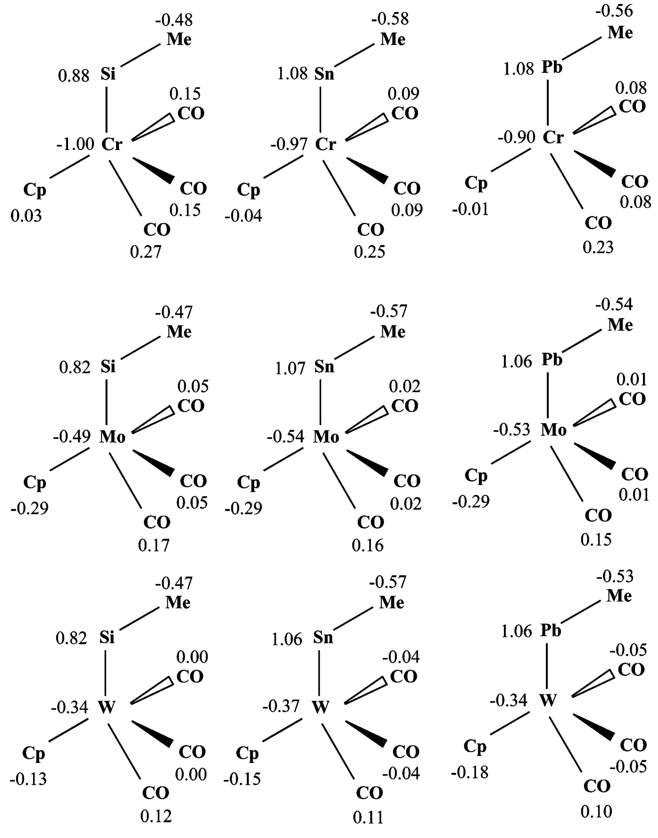

Figure 5. Calculated NBO partial charges of the metallo-ylidene complexes **IIa**-**IIi**.

of the d character in the metal atoms along the M≡E σ bonds is shown in Figure 6. It becomes obvious that the % d contribution of the metal atoms along the M≡E σ bonds for the complexes **Ia**−**Ii** is much lower than for the compounds **IIa**−**IIi**. Hence, there will be stronger interactions between M sd$_\sigma$ orbitals and E spσ orbitals for the compounds **IIa**−**IIi** than for the compounds **Ia**−**Ii**.

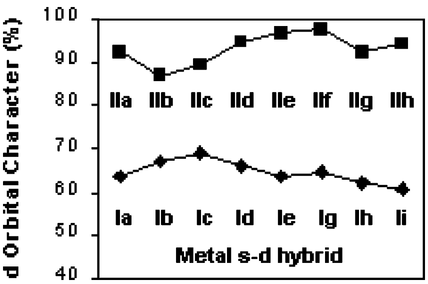

Figure 6. Metal d orbital character (%) along M−E bond in $[(\eta^5\text{-}C_5H_5)(CO)_2M{\equiv}EMe]$ (**Ia**−**Ii**) and $[(\eta^5\text{-}C_5H_5)(CO)_3M{-}EMe]$ complexes (**IIa**−**IIh**).

To visualize the differences in the linear M≡E−R and bent M−E−R bonding between **Ia**−**Ii** and **IIa**−**IIi**, envelope plots of some relevant molecular orbitals of the molybdenum-silylidyne complex $[(\eta^5\text{-}C_5H_5)(CO)_2Mo{\equiv}SiMe]$ **Id** and the molybdenum-silylidene compound $[(\eta^5\text{-}C_5H_5)(CO)_3Mo\text{-}SiMe]$ **IId** are shown in Figure 7.

Figures 7a (HOMO-1) and 7b (HOMO-2) give a pictorial description of the Mo−Si π bonding, while Figure 7c (HOMO-4) shows mainly the Mo−Si−C σ bonding orbital in the complex **Id**. The HOMO-1 has a′ (σ) symmetry and HOMO-2 has a″ (π) symmetry. However, the shape of the orbital shows clearly that the HOMO-1 can be identified with the π component of the π back-donation (Figure 1a). The HOMO (Figure 7d) of **IId** is mainly the lone pair orbital at Si, which has, however, some in plane pseudo π bonding contributions. Figure 7e (HOMO-4 of **IId**) shows mainly the Mo−Si σ-bonding orbital. The LUMO (Figure 7f) of **IId** is mainly non-bonding p$_\pi$ orbital at Si. Hence, the HOMO and HOMO-4 orbitals of **IId** may be compared with the σ bonding components of the qualitative orbital model (Figure 1b). We note that there is no true π bonding orbital in **IId**. Similar molecular orbitals have been observed for metal-stannylidyne, metal-plumbylidyne complexes, and metallostannylidene, metalloplumbylidene compounds. It becomes clear that the complexes **Ia**−**Ii** have a large contribution from π bonding orbitals, while **IIa**−**IIi** are σ compounds. It is important to note that there are two σ(a′) bonding orbitals in the compounds **IIa**−**IIi** but only one in **Ia**−**Ii**. This is an explanation for the finding that the σ(a′) interactions in compounds II are more important than those in I, as pointed out by the EDA analysis, considering both charged and neutral fragments.

Summary and Conclusion

A theoretical study has been presented where the bonding situation in silylidyne, stannylidyne, plumbylidyne complexes and metallosilylidenes, metallostannylidenes, metalloplumbylidenes are compared with each other. The calculated geometries are in excellent agreement with available experimental values. The WBI values of the M≡E bonds in the complexes having linear M≡E−R linkage, **Ia**−**Ii** are significantly higher (1.23−1.64) than the WBI values of the M−E bonds in the compounds having bent M−E−R linkage, **IIa**−**IIi** (0.32−0.74). The latter values are approximately one-third of the WBI values of the M≡E bonds. The nature of the M≡EMe and M−EMe interactions was analyzed with charge and energy decomposition methods. In the M≡EMe bond, the M−E σ-bonding orbitals are always polarized

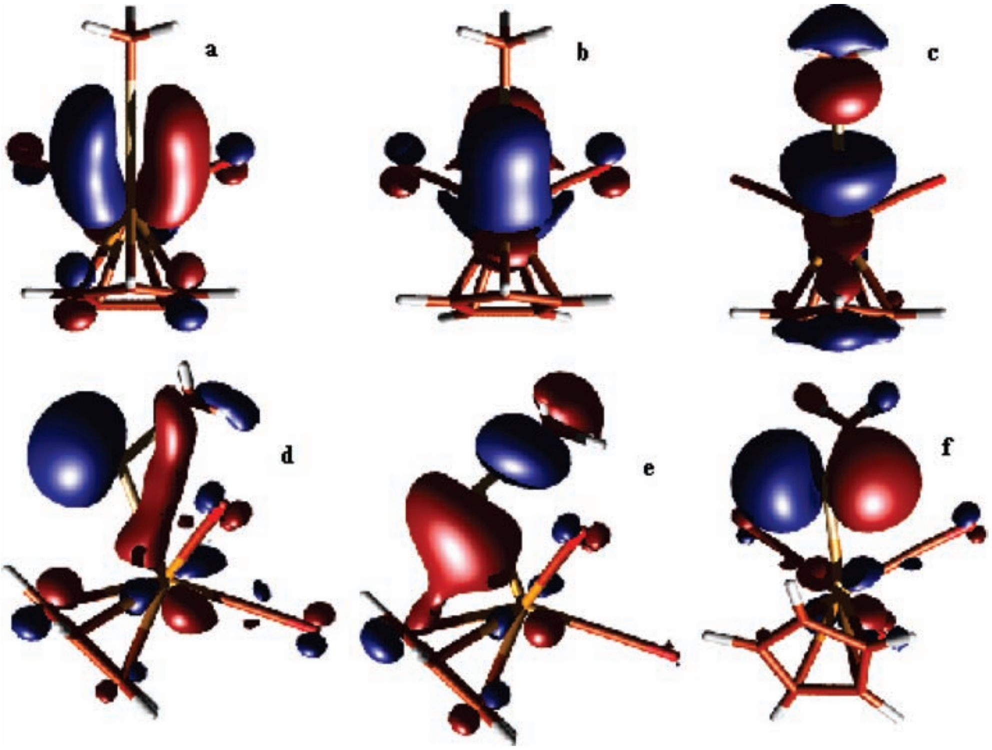

Figure 7. Plot of some relevant orbitals of $[(\eta^5\text{-}C_5H_5)(CO)_2M{\equiv}SiMe]$ **Id** (a, b, c) and $[(\eta^5\text{-}C_5H_5)(CO)_3M\text{-}SiMe]$ **IId** (d, e, f).

toward the silicon, tin, and lead atoms and the polarization increases from chromium to tungsten. In contrast, in the M−EMe bond, the M−E σ-bonding orbitals are significantly polarized toward the metal atom. The hybridization at the metal atoms in the M≡E bonds has d character in the range 60.6−68.8%, while the M−E bonds have large d character which is always >86% of the total atomic orbital contribution. In the complexes **Ia**−**Ii**, the contributions of the electrostatic interactions, ΔE_{elstat}, and the covalent bonding, ΔE_{orb}, have nearly the same values for silylidyne and germylidyne complexes, while for the stannylidyne and plumbylidyne complexes, the electrostatic interactions, ΔE_{elstat}, are greater than the orbital interactions, ΔE_{orb}. The covalent bonding has a high degree of π-character. The total interaction energies ΔE_{int} in the compounds **IIa**−**IIi** are less attractive than those in the complexes **Ia**−**Ii**. The M−ER bonds have a slightly lower degree of covalent bonding (34.9−44.9%) than the M≡EMe bonds (42.1−50.2%). The drastic difference between the two classes of compounds are found for the degree of a″ (π) bonding. The contribution of ΔE_{π} to the covalent term ΔE_{orb} is much higher in the M≡EMe bonding (41.6−42.6%) than in the M−EMe bonding (17.1−20.4%). While the π bonding contributions in $[(\eta^5\text{-}C_5H_5)(CO)_3M{-}EMe]$ are weaker than those in $[(\eta^5\text{-}C_5H_5)(CO)_2M{\equiv}EMe]$, the σ-bonding contribution in the former compounds are stronger than those in the latter.

Acknowledgment. We thank Professor Gernot Frenking, Philipps-Universität Marburg, for helpful suggestions. Financial support from the Spanish MICINN (Project Consolider Ingenio 2010 CSD2007-00006) and Generalitat de Catalunya ("Distinció per a la Promoció de la Recerca Universitaria 2004" and 2005SGR 00896) is gratefully acknowledged.

Supporting Information Available: Optimized structures of **Ia**−**IIi.** Tables with the Cartesian coordinates of the optimized geometries of **Ia**−**IIi**. NBO Analysis of the π bonds in the metal-ylidyne complexes. This material is available free of charge via the Internet at http://pubs.acs.org.

IC801072G